

# **E12-10-008 Update: Detailed studies of the nuclear dependence of $F_2$ in light nuclei.**

J. Arrington

*Argonne National Laboratory, Argonne, IL*

D. Gaskell

*Jefferson Laboratory, Newport News, VA*

A. Daniel

*Ohio University, Athens, OH*

**Spokespersons,  
for the E12-10-008 collaboration.**

(Dated: June 30, 2010)

## **Abstract**

Jefferson Lab experiment E12-10-008 was approved to perform inclusive electron scattering measurements from several light to medium heavy nuclei over a broad range of  $x$  ( $0.1 < x < 1$ ) up to  $Q^2 \approx 15 \text{ GeV}^2$ . The data collected by this experiment will build on existing JLab measurements of the EMC effect by extending precise extraction of the EMC ratios to a larger  $x$  and  $Q^2$  range, and by making additional measurements on light nuclei ( $A < 12$ ) to provide better data for constraining calculations of nuclear effects in these well understood nuclei. Because results from Jefferson Lab do not support the previous  $A$ -dependent or density-dependent fits to the EMC effect, including an expanded set of light nuclei will help investigate the role of the detailed nuclear structure and test the idea that the *local* nuclear environment plays an important role in the modification of quark distributions. In addition, a better understanding of the EMC effect in light nuclei will provide guidance for calculation of nuclear effects in deuterium, which is necessary to extract the neutron structure function, while new measurements of the deuteron and proton structure functions at large  $x$  will provide new data for such extractions.

This document briefly summarizes the motivation and requirements of the experiment E12-10-008. The physics motivation for the measurements remains essentially unchanged, and there have been no major changes in any technical aspects of the experiment since it was approved by PAC35. For the full version of the proposal please see reference [1].

## I. SCIENTIFIC MOTIVATION

Conventional nuclear physics describes nuclei as clusters of protons and neutrons held together by a strong force mediated by meson exchange. However, protons and neutrons are not the fundamental degrees of freedom of the underlying theory, quantum chromodynamics (QCD). The modification of hadron properties in the nuclear environment is of fundamental importance in understanding the implications of QCD for nuclear physics. One of the most important nuclear medium effect is the European Muon Collaboration (EMC) effect [2]. The EMC collaboration found significant deviation between the structure functions of heavy (iron) and light (deuterium) nuclei. Since then, the nuclear dependence of structure functions has been extensively studied, both experimentally and theoretically (see Refs. [3–6]). However, despite the large body of data available, there is as yet no clear consensus on origin of the EMC effect. Though the measurements of the EMC effect are a clear signature of nuclear quark-gluon effects, the complete explanation for this modification is theoretically difficult to isolate, since purely hadronic effects such as binding, Fermi motion and other possible nuclear corrections may all be contributing.

SLAC E139 [3] mapped out the high  $x$  region for a range of nuclei, yielding a measurement of the  $A$  dependence of the EMC effect. While the general  $x$  dependence and  $A$  dependence of the EMC effect were relatively well mapped out, they did not provide sufficiently strong constraints on the models of the EMC effect, nor could they differentiate between scaling of the EMC effect with nuclear mass or density.

## II. RESULTS FROM E03-103

JLab experiment E03-103 addressed some of these limitations in previous measurements of the EMC effect. The primary goal was to make improved measurements of the EMC effect, focusing on large  $x$ , where Fermi motion and binding are believed to be the dominant effects, and for light nuclei, where the uncertainties in the nuclear structure are smaller, thus reducing uncertainties in comparisons to calculations of the EMC effect. The measurement provided benchmark data for calculations of the EMC effect in light nuclei, as well as providing direct measure of the  $A$  dependence of the EMC effect in light nuclei [7]. We provide a very brief overview of the results from the 6 GeV measurement.

- While the 6 GeV measurement was at somewhat lower  $Q^2$  values than SLAC E139 (which took data mainly at 5 and 10 GeV<sup>2</sup>), we obtained high precision at larger  $x$  values by making measurements at somewhat lower  $W^2$  values. Data were also taken at several energy and angle settings, to map out the  $Q^2$  dependence of the ratios and cross sections in detail, allowing us to verify that our data were interpretable in the context of quark distributions in nuclei. As seen in Figure 1, the high  $Q^2$  settings show no systematic  $Q^2$  dependence in the ratios, and set significant limits on the  $Q^2$  dependence up to  $x \approx 0.85$ . The main results from the experiments are taken from the  $Q^2 = 5.33$  GeV<sup>2</sup> setting.

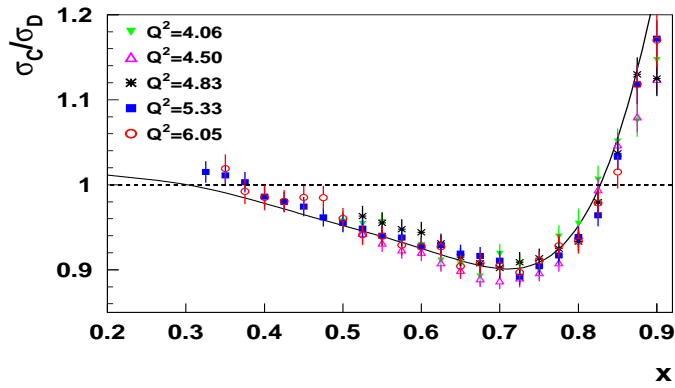


FIG. 1: The E03-103 EMC ratios for carbon [7], from the five largest  $Q^2$  settings. The  $Q^2$  values quoted correspond to  $x = 0.75$ , and the curve is the SLAC parametrization.

- E03-103 provided the first measurement of the EMC effect for  ${}^3\text{He}$  in the valence region, as well as significantly improved data on  ${}^4\text{He}$ . The EMC effect in  ${}^3\text{He}$  is significantly smaller than that in  ${}^4\text{He}$ , as seen in Fig. 2. This provides benchmark data for models of the EMC effect, allowing comparison to few-body nuclei with well understood structure, as well as providing high precision data at larger  $x$  values than were available from the SLAC measurements.

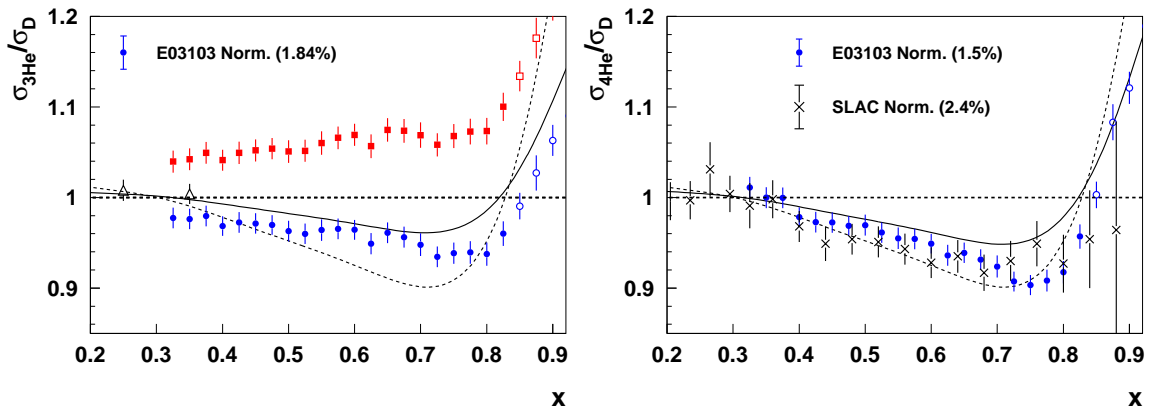


FIG. 2: The E03-103 results [7] for  ${}^3\text{He}$  (left) and  ${}^4\text{He}$  (right). For  ${}^3\text{He}$ , the red squares show the measured cross section ratio, and the blue circles are after applying the isoscalar correction. The dashed (solid) curve is the SLAC fit to the EMC effect for carbon (helium). Hollow symbols indicate data at  $x \geq 0.85$  ( $W^2 \leq 2 \text{ GeV}^2$ ).

- To minimize the impact of normalization uncertainties, of particular importance for the cryogenic helium isotopes, we use the difference between the ratio at small and large  $x$  values as a measure of the size of the EMC effect. In particular, we fit the region  $0.35 < x < 0.7$  to a straight line, and use the slope as a measure of the size of the nuclear effects. Fig. 3 shows the  $A$  dependence of the extracted EMC effect for the  $A \leq 12$  nuclei. The difference between  ${}^3\text{He}$  and  ${}^4\text{He}$  is much larger than predicted by the SLAC  $A$ -dependent parametrization, while the large EMC effect in  ${}^9\text{Be}$  contradicts the density-dependent parameterizations. Because  ${}^9\text{Be}$  has a significant cluster

structure, mainly two tightly bound alpha particles plus an extra neutron, most of the nucleons and all of the protons are in a dense local environment. Thus, the observed  $A$  dependence suggests that clustering effects are important, as it may be the local environment of the nucleons that leads to the modification of the structure function.

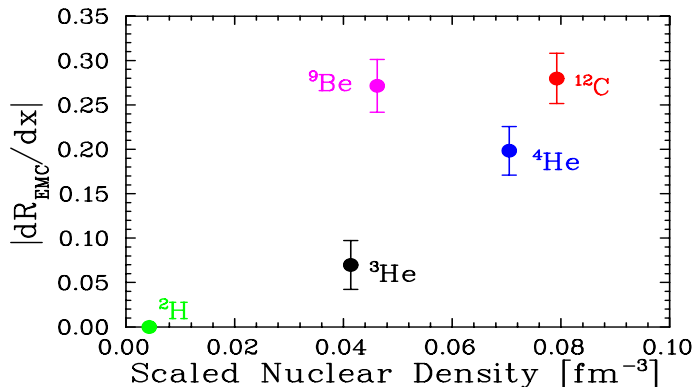


FIG. 3: Slope of the isoscalar EMC ratios for  $0.35 < x < 0.7$  as a function of scaled nuclear density [7].

### III. PROPOSED MEASUREMENTS

The results from E03-103 emphasize the need for precise measurements on a range of well understood nuclei. This is one of the main motivations of the proposed experiment. In addition, measurements at higher beam energy will reduce the uncertainty related to the isoscalar correction for  $^3\text{He}$  and allow for better comparisons of the  $x$  dependence of the EMC effect in light nuclei. Finally, the use of  $^{40}\text{Ca}$  and  $^{48}\text{Ca}$  will provide a first test of models which predict a significant flavor dependence in the EMC effect.

The kinematics of E03-103 and for the proposed measurements are shown in Fig. 4. These measurements will extend coverage in the DIS region from  $x = 0.6$  to  $x = 0.8$ , while measurements for  $W^2 > 2 \text{ GeV}^2$ , where precise  $Q^2$  independence was observed at 6 GeV, will be extended to  $x = 0.92$ . Extending the measurements down to  $x \approx 0.1$  will let us better compare the shape ( $x$  dependence) of the EMC effect in these nuclei. This is especially important for some of the light nuclei, where the the normalization uncertainties become a limiting factor in determining the size of the EMC effect at large  $x$ . Finally, the increased  $Q^2$  range at large  $x$  will allow us to extract  $^3\text{He}/(^2\text{H}+^1\text{H})$ , which allows for a EMC-like measurement on  $^3\text{He}$  that is independent of the large isoscalar correction shown in Fig. 2. While this was measured at 6 GeV, the proton resonance structure leads to structure in this EMC ratio above  $x \approx 0.65$ , which will be dramatically reduced for the proposed 11 GeV measurements, as seen in Fig. 5. Thus, the data on  $^3\text{He}$  can be precisely compared to detailed calculations up to  $x = 0.85$ , without the uncertainty associated with knowledge of the neutron structure function.

In addition to the expanded kinematic coverage possible with 11 GeV, we will also provide data on additional light nuclei, including nuclei with significant clustering behavior, to better

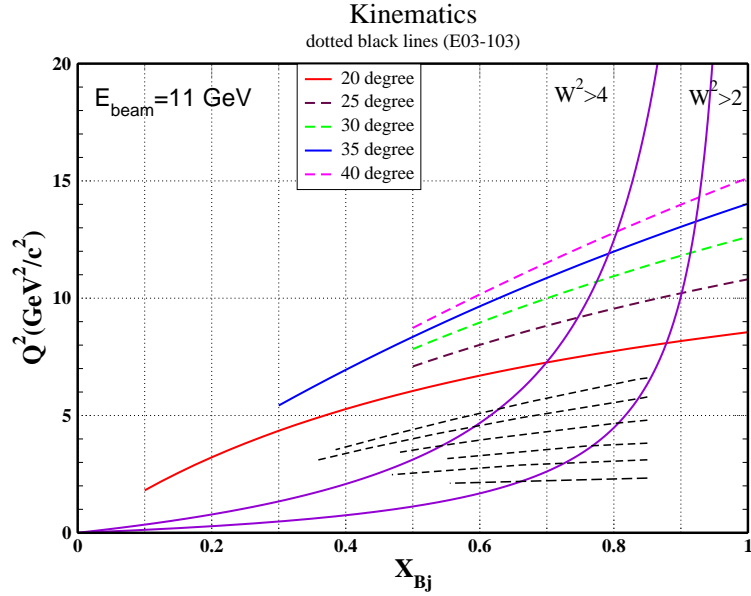


FIG. 4: Overview of the proposed kinematics. The black dotted lines are the kinematics from E03-103, and the solid red and blue lines (20 and 35 degrees) are the primary kinematics for the proposed EMC effect measurements. Data on a small subset of targets at additional angles will be used to study the  $Q^2$  dependence of the ratios (dashed lines). The solid purple lines correspond to contours of fixed  $W^2$  values.

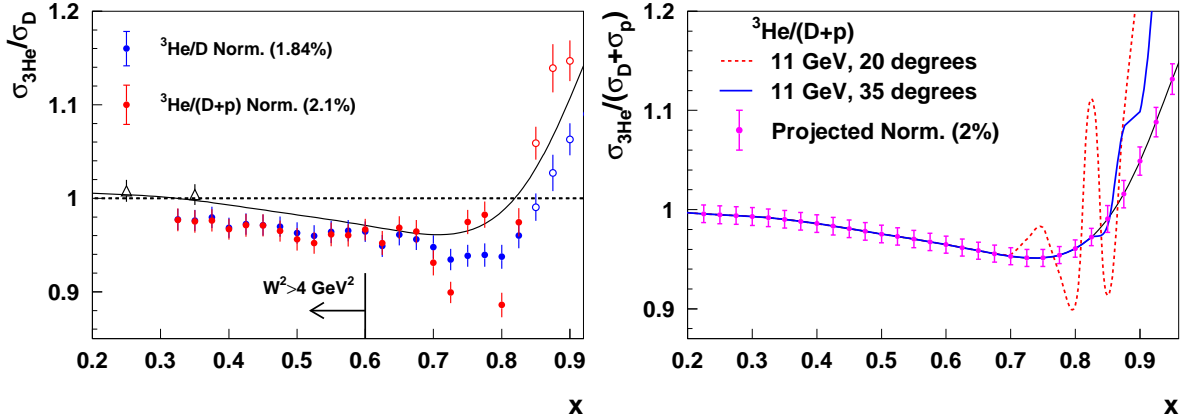


FIG. 5: The left right panel shows the isoscalar-corrected  ${}^3\text{He}/{}^2\text{H}$  ratios (blue points) and the  ${}^3\text{He}/({}^2\text{H}+{}^1\text{H})$  ratio (red points) from E03-103. The black curve is the SLAC A dependent fit to  ${}^3\text{He}$ . The right panel shows the projected uncertainties for the  ${}^3\text{He}/({}^2\text{H}+{}^1\text{H})$  ratios, along with a model for this ratio including the contributions from the proton resonance structure at 20 and 35 degrees. Note that the structure in the ratios (due to the proton resonance contribution) shrinks and gets pushed to higher  $x$  values at larger  $Q^2$ .

map out the A dependence of the EMC effect. While  ${}^4\text{He}$  and  ${}^9\text{Be}$  are sensitive to the difference between scaling with A and density,  ${}^6\text{Li}$  and  ${}^7\text{Li}$  yield large differences between scaling with A and with *local* density. The local density parameter comes from the GFMC calculations of the two body density (the distribution of N–N separation in the nuclei). We integrate the short distance part of the two body density using a gaussian cutoff, as an

measure of the nearby density (neglecting the nucleon itself). This can also be thought of as a measure of the amount of overlap between nearby nucleons. Data on this collection of light nuclei will shed additional light on the scaling and the microscopic origin of the EMC effect.

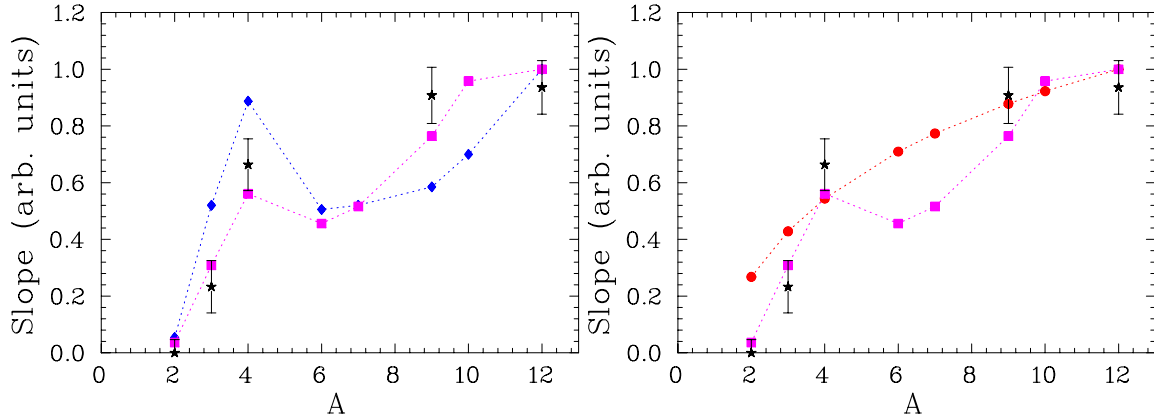


FIG. 6: The magnitude of the EMC effect for different light nuclei from E03-103 (black stars) and predictions based on simple scaling prescriptions. The blue diamonds scale the EMC effect with density, and the red circles scale as  $A^{1/3}$ . The magenta squares represent the results using the local density as discussed in the text.

One entirely new aspect of this measurement is the ability to look for a flavor dependence to the EMC effect. There have been recent suggestions of a significant isospin-dependence for the EMC effect [8, 9]. Measurements of  $^{40}\text{Ca}$  and  $^{48}\text{Ca}$  will provide a significant variation of the n/p ratio in the nucleus, while maintaining a comparison between nuclei of similar mass and density. In the model by Cloet et al, a neutron or proton excess in nuclei generates an isovector mean field which, through its coupling to the quarks in a bound nucleon, creates a shift in the quark distributions. The isospin dependence of the interaction leads to different degree of modification for the up and down quark distributions, yielding a difference in the EMC effect for these nuclei as shown in Fig. 7.

Finally, the additional several light nuclei will provide secondary benefits. Comparisons of nuclei which differ by just one nucleon (for example  $^{11}\text{B}$ - $^{10}\text{B}$ ,  $^7\text{Li}$ - $^6\text{Li}$ ,  $^{12}\text{C}$ - $^{11}\text{B}$ ) will allow the extraction of the structure function of a single nucleon in the nucleus. This can be used to a check the isoscalar corrections applied in these nuclei. Direct measurements of the EMC effect in  $^6\text{Li}$  and  $^7\text{Li}$  are useful for polarized LiH or LiD targets, where the EMC effect modifies the dilution factor. In addition, plans are being made to measure the spin EMC effect using  $^7\text{Li}$ , and having a high precision measurement of the unpolarized EMC effect will help separate out spin-dependent effects from contributions which have the same impact on the spin-dependent and spin-independent quark distributions.

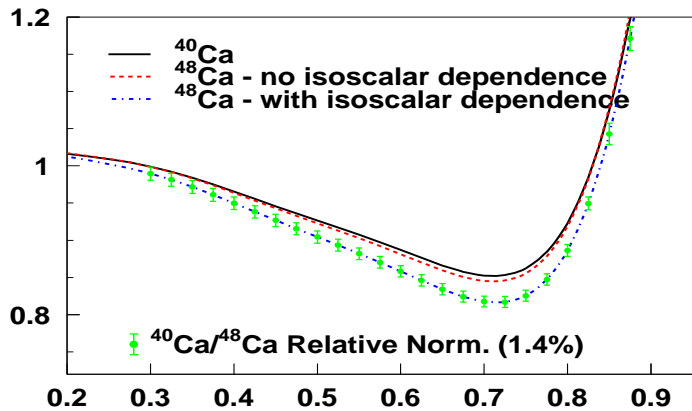


FIG. 7: The figure shows projected uncertainties in the  $^{48}\text{Ca}$  EMC ratios. The black and red curves represent the EMC ratios calculated using the SLAC A-dependent parametrization. The blue curve represents the results of the calculations using the QMC model [8]. In the calculation, the densities are fixed to nuclear matter densities and the results are scaled down to match the  $N/Z$  for  $^{48}\text{Ca}$ .

#### IV. DETAILS OF THE PROPOSED MEASUREMENTS

The kinematics are shown in Fig. 4. We will measure inclusive electron scattering from hydrogen, deuterium,  $^3\text{He}$ ,  $^4\text{He}$ ,  $^{6,7}\text{Li}$ ,  $^9\text{Be}$ ,  $^{10,11}\text{B}$ ,  $^{12}\text{C}$ ,  $^{40,48}\text{Ca}$ , and  $^{63}\text{Cu}$ , along with measurements on an aluminum target for subtraction of the cryotarget endcap contributions.

For most of the targets, data will be taken at 20 degrees, as this allows measurements down to  $x = 0.1$  while avoiding large pion backgrounds, charge symmetric backgrounds, and radiative corrections. For nuclei where it is important to push to the largest  $x$  values, we will take data at 35 degrees, to maximize the  $Q^2$  while maintaining low backgrounds down to  $x = 0.3$ . The primary cases where large  $x$  is important are the comparison of  $^{40}\text{Ca}$  and  $^{48}\text{Ca}$  and the  $^3\text{He}$  ratios, where forming the ratio  $^3\text{He}/(^2\text{H}+^1\text{H})$  allows comparisons to calculations that are independent of the neutron structure function. The choice of the kinematics for the proposed experiment are based on our experience with the E03-103 analysis and are chosen to provide a significant coverage in  $x$  and  $Q^2$  while minimizing backgrounds and radiative corrections.

The main background of concern is secondary electrons coming from pair production in the target. Based on parameterizations of the charge symmetric background and our results from E03-103, these should be of concern only at low  $x$  and high  $Q^2$  values. We have chosen our angles such that this background is small, except for the lowest  $x$  values ( $x = 0.1$  at 20 degrees,  $x = 0.3$  at 35 degrees), and we will make measurements of this background by running in positive polarity, as was done for E03-103. The low  $x$ , large  $Q^2$  region is also where radiative corrections from quasielastic scattering become large, and by taking data at relatively modest scattering angles, these contributions are relatively small, even at the lowest  $x$ . Details on all of these corrections are included in the full proposal [1].

Table I is a summary of the estimated beam time required for the measurement. Details

| Activity   | Time (hours)   |
|--|----------------|
| Production Running (incl. dummy)                               | 406            |
| Positron runs  | 24             |
| Checkout/calibration   | 24             |
| Kinematic changes  | 28             |
| ${}^1,2\text{H} \rightarrow {}^3,4\text{He}$ Target changeover | 24             |
| Target Boiling Studies   | 16             |
| Hydrogen elastics  | 16             |
| BCM calibrations   | 8              |
| Radiative corrections check                                    | 8              |
| <b>Total</b>   | <b>23 days</b> |

TABLE I: Beam time required for the proposed experiment. The time shown is for SHMS and HMS taking data simultaneously.

of the time estimate is discussed in appendix A. We estimate that 23 days in Hall C will be required to carry out the measurements in the proposal.

## V. SUMMARY

E12-10-008 will measure inclusive scattering from  ${}^1,2\text{H}$ ,  ${}^3,4\text{He}$ ,  ${}^6,7\text{Li}$ ,  ${}^9\text{Be}$ ,  ${}^{10,11}\text{B}$ ,  ${}^{12}\text{C}$ ,  ${}^{40,48}\text{Ca}$ , and  ${}^{63}\text{Cu}$  for  $0.1 < x < 1$ . Though a considerable body of data has been accumulated on nuclear parton distributions, the precise data from the proposed experiment will provide stringent constraints on the physics underlying nuclear dependence of parton distribution functions.

The high  $x$  measurements on a range of well understood light nuclei will provide a comprehensive and precise basis to test state of the art models that attempt to explain the observed nuclear dependence. Since the conventional nuclear effects lead to modifications of the structure functions at all  $x$  values, a quantitative understanding is important before the addition of more exotic effects which may be required to explain the low  $x$  behavior. The unusual  $A$ -dependence observed in light nuclei in our previous experiment can be better studied with the addition of high precision measurements on additional light nuclei and more detailed comparisons of the  $x$  dependence of the EMC effect in few-body nuclei. Finally, we will make a comparison of the EMC effect in  ${}^{40}\text{C}$  and  ${}^{48}\text{Ca}$ , which will, for the first time, be able to directly constrain the flavor dependence of the EMC effect, e.g. as proposed in recent calculations [8].

## APPENDIX A: DETAILS OF THE BEAM TIME REQUEST

All data taking for E12-10-008 is at 11 GeV beam energy. Figure 4 shows the proposed kinematic coverage as a function  $x$  and  $Q^2$ . Data from 20 and 35 degrees will be used for



| Target           | 35 deg<br>(SHMS) | 20 deg<br>(HMS) | 25 deg<br>(HMS) | 30 deg<br>(HMS) | 40 deg<br>(HMS) | 40deg<br>(SHMS) | total HMS<br>time | total SHMS<br>time |
|------------------|------------------|-----------------|-----------------|-----------------|-----------------|-----------------|-------------------|--------------------|
| <sup>1</sup> H   | 39.6             | 2.8             | 5.4             | 15.7            | 40.1            | 24.6            | 64.0              | 64.2               |
| <sup>2</sup> H   | 28.2             | 2.6             | 3.9             | 10.8            | 29.5            | 19.0            | 46.8              | 47.2               |
| <sup>3</sup> He  | 35.0             | 1.9             |                 |                 | 46.2            | 14.4            | 48.1              | 49.4               |
| <sup>4</sup> He  | 18.0             | 1.8             |                 |                 |                 |                 | 1.8               | 18.0               |
| <sup>6</sup> Li  |                  | 5.4             |                 |                 |                 |                 | 5.4               |                    |
| <sup>7</sup> Li  | 82.9             | 4.5             |                 |                 |                 |                 | 4.5               | 82.9               |
| <sup>9</sup> Be  |                  | 1.6             |                 |                 |                 |                 | 1.6               |                    |
| <sup>10</sup> B  | 18.8             |                 |                 |                 |                 |                 |                   | 18.8               |
| <sup>11</sup> B  | 18.8             |                 |                 |                 |                 |                 |                   | 18.8               |
| <sup>12</sup> C  | 18.8             | 1.6             | 1.6             | 5.3             | 16.7            | 6.8             | 25.2              | 25.6               |
| <sup>40</sup> Ca | 34.7             |                 |                 |                 |                 |                 |                   | 34.7               |
| <sup>48</sup> Ca | 24.3             |                 |                 |                 |                 |                 |                   | 24.3               |
| <sup>63</sup> Cu |                  | 1.6             |                 |                 |                 |                 | 1.6               |                    |
| Total            | 319              | 24              | 11              | 32              | 132.5           | 65              | 199               | 383.9              |

TABLE II: Detailed breakdown of the kinematic settings and approximate run times (in hours) needed for each target at a given setting.

the main EMC ratio extraction. Data on a small subset of targets at additional angles (as indicated in the figure) will be used to study the  $Q^2$  dependence of the ratios to precisely define the region of scaling.

We will run at currents between 15 and  $80\mu\text{A}$  ( $15\mu\text{A}$  for the <sup>6,7</sup>Li targets,  $30\mu\text{A}$  for the <sup>40,48</sup>Ca targets). Run times have been estimated assuming 0.5% statistics in each  $x$  bin for  $W^2 > 3$  and at least 1% statistics for  $3 > W^2 > 2$  for each target (double the statistics for deuterium, which generally has a shorter run time). Note that for the <sup>7</sup>Li running at the highest  $x$  and largest  $Q^2$ , we will take about half the typical statistics due to the need to run at low currents. The planned settings and the time needed to acquire the proposed statistical accuracy are shown in table II. Scattered electrons will be measured in the HMS and SHMS spectrometers, which will run simultaneously, but independently. The run times are calculated by assuming 6.5msr acceptance for the HMS and 5msr for the SHMS. Approximately 384 hours is needed for the data acquisition on SHMS while 199 hours is needed for the HMS running. Since the spectrometers are taking data simultaneously, we have planned the running to maximize the overlap and efficiency for the two spectrometers. However, there are a few settings and targets that will only be used for the HMS and can not be taken concurrently with SHMS running. This adds an extra 8.6 hours to the total 384 hours for the SHMS run time. Hence, we estimate that a total production time of 392.5 hours will be required. Since the dummy aluminum target will be used to directly measure the cell wall contribution to the total yield, this requires an additional 14 hours of beam

| Setting     | $x$ range<br>(for $W^2 > 2$ ) | Number of<br>momentum<br>changes | Time for<br>momentum<br>changes | Number of target<br>changes per<br>momentum setting | Total time<br>for target<br>changes |
|-------------|-------------------------------|----------------------------------|---------------------------------|---|-------------------------------------|
| SHMS 35 deg | 0.3–0.92                      | 4                                | 2.7*                            | 11  | 3.7                                 |
| SHMS 40 deg | 0.5–0.93                      | 3                                | 2.0*                            | 5   | 1.2                                 |
| HMS 20 deg  | 0.1–0.87                      | 7                                | 4.7*                            | 10  | 5.8                                 |
| HMS 25 deg  | 0.5–0.9                       | 3                                | 1.0                             | 3   | 0.7                                 |
| HMS 30 deg  | 0.5–0.91                      | 3                                | 1.0                             | 3   | 0.7                                 |
| HMS 40 deg  | 0.5–0.93                      | 4                                | 2.7*                            | 5   | 1.7                                 |
| Total time  |                               |                                  | 14.1                            |   | 13.8                                |

TABLE III: Time required (in hours) needed for the kinematic and target change. Settings with an asterisk involve kinematics where the time for the momentum changes has been double, as the momentum scan has to be performed with  $^1\text{H}$  cryotargets and again with  $^3,4\text{He}$  cryotargets.

time (with simultaneous data taking in the HMS and SHMS). Thus the total beam on time is estimated to be 406 hours.

Table III shows the detailed estimate of the extra time (in hours) required for the kinematic and target changes. Based on the previous experience we estimate that roughly 20 minutes is needed for a momentum change, 10 minutes for angle change and 5 minutes for target change. Since the  $^1,2\text{H}$  and the  $^3,4\text{He}$  cannot run at the same time in the present target configuration in Hall C, we add an additional 24 hours for the target changeover. For the settings with  $^1,2\text{H}$  and  $^3,4\text{He}$  we plan to do dummy runs twice and a carbon run for cross checks. Including time for checkout, hydrogen elastics studies, BCM calibrations, etc. makes the total beam time to 23 days as summarized in table I.

- 
- [1] J. Arrington, A. Daniel, and D. Gaskell, spokespersons, Jefferson lab experiment E12-10-008, [http://www.jlab.org/exp\\_prog/proposals/10/PR12-10-008.pdf](http://www.jlab.org/exp_prog/proposals/10/PR12-10-008.pdf).
  - [2] J. J. Aubert et al., Phys. Lett. B **123**, 123 (1983).
  - [3] J. Gomez et al., Phys. Rev. D **49**, 4348 (1994).
  - [4] D. F. Geesaman, K. Saito, and A. W. Thomas, Ann. Rev. Nucl. Part. Sci. **45**, 337 (1995).
  - [5] P. R. Norton, Rept. Prog. Phys. **66**, 1253 (2003).
  - [6] M. Arneodo, Phys. Rep. **240**, 301 (1994).
  - [7] J. Seely et al., Phys. Rev. Lett. **103**, 202301 (2009).
  - [8] I. C. Cloet, W. Bentz, and A. W. Thomas, Phys. Lett. **B642**, 210 (2006).
  - [9] M. Hirai, S. Kumano, and T.-H. Nagai, Phys. Rev. **C76** (2007).